ACS APPLIED MATERIALS & INTERFACES

Research Article

www.acsami.org

REDV Peptide Conjugated Nanoparticles/pZNF580 Complexes for Actively Targeting Human Vascular Endothelial Cells

Changcan Shi,[†,‡] Qian Li,[†] Wencheng Zhang,[§] Yakai Feng,*[,†,∥,⊥,#] and Xiangkui Ren*[,†,∥]

[†]School of Chemical Engineering and Technology, Tianjin University, Tianjin 300072, China

[‡]Wenzhou Institute of Biomaterials and Engineering, Wenzhou 325011, China

[§]Department of Physiology and Pathophysiology, Logistics University of Chinese People's Armed Police Force, Tianjin 300162, China

[∥]Joint Laboratory for Biomaterials and Regenerative Medicine, Tianjin University-Helmholtz-Zentrum Geesthacht, Tianjin 300072, China

[⊥]Collaborative Innovation Center of Chemical Science and Chemical Engineering (Tianjin), Tianjin 300072, China

[#]Key Laboratory of Systems Bioengineering of Ministry of Education, Tianjin University, Tianjin 300072, China

Supporting Information

ABSTRACT: Herein, we demonstrate that the REDV peptide modified nanoparticles (NPs) can serve as a kind of active targeting gene carrier to condensate pZNF580 for specific promotion of the proliferation of endothelial cells (ECs). First, we synthesized a series of biodegradable amphiphilic copolymers by ring-opening polymerization reaction and graft modification with REDV peptide. Second, we prepared active targeting NPs via self-assembly of the amphiphilic copolymers using nanoprecipitation technology. After condensation with negatively charged pZNF580, the REDV peptide modified NPs/pZNF580 complexes were formed finally. Due to the binding affinity toward ECs of the specific peptide, these REDV peptide modified NPs/pZNF580 complexes could be recognized and adhered specifically by ECs in the coculture system of ECs and human artery smooth muscle cells (SMCs) *in vitro*. After expression of ZNF580, as the key protein to promote the proliferation of ECs, the relative ZNF580 protein level increased from 15.7% to 34.8%. The specificity in actively targeting ECs of the REDV peptide conjugated NPs/pZNF580 complexes was still retained in the coculture system. These findings in the present study could facilitate the development of actively targeting gene carriers for the endothelialization of artificial blood vessels.

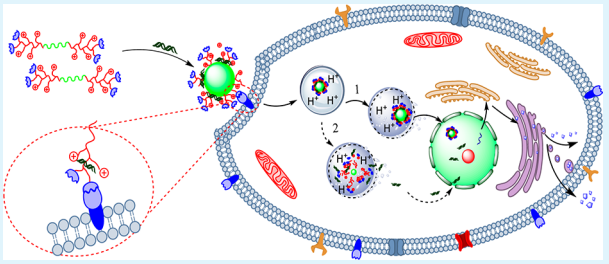

KEYWORDS: *REDV peptide, gene carriers, actively targeting, nanoparticles, endothelial cells, proliferation*

1. INTRODUCTION

With the high occurrence of cardiovascular diseases, there is a constant high demand of vascular grafts that can provide long-term patency for replacement therapy.[1] During the clinical application, synthetic artificial vascular grafts with inner diameters larger than 6 mm are frequently used for bypass grafts or replacements, and they provide good, long-term clinical patency.[2] However, small-caliber vascular grafts (<6 mm) often cannot achieve long-term patency due to acute thrombogenicity on the luminal surface and occlusion.[3]

Many strategies are used to enhance the hemocompatibility of artificial blood vessels.[2] For example, in order to improve the surface hydrophilicity of polymeric artificial blood vessels, collagen,[4] heparin,[5] poly(ethylene glycol),[6−10] gelatin,[11,12] 2-methacryloyloxyethyl phosphorylcholine,[13,14] zwitterionic polynorbornene,[15] and silk fiber[16,17] have been widely used in surface modification of artificial blood vessels by us and other research groups. Through surface modification, the hydrophilicity, hemocompatibility, and biocompatibility of the artificial blood vessels are improved significantly.[18]

In the prevention of the occlusion of the natural blood vessels, it is a fact, which should not be ignored, that endothelium plays an important role.[19] Therefore, on the luminal surface of small-caliber vascular grafts, rapid endothelialization is a smart strategy to inhibit the initial thrombosis and facilitate better long-term patency.[20] In order to create a bioactive surface with ECs capturing and/or binding capability, Arg-Gly-Asp (RGD) and Arg-Glu-Asp-Val (REDV) peptides are usually used as ligands to adhere ECs for rapid endothelialization.[21] Furthermore, REDV peptide exhibits specific EC adsorption, because REDV peptide as the active targeting ligand can be recognized by $\alpha_4\beta_1$ integrin receptor that is expressed specifically on the cytomembrane of ECs.[22] Therefore, when biomaterial surface was modified by REDV peptide, the surface showed efficiently selective EC adhesion.[23] Moreover, when stents are coated with phosphorylcholine and

Received: July 13, 2015
Accepted: August 28, 2015
Published: September 3, 2015

DOI: 10.1021/acsami.5b06286
ACS Appl. Mater. Interfaces 2015, 7, 20389−20399

REDV peptides, they exhibited high EC selectivity compared with other cell types *in vivo*.[24]

In order to promote the proliferation and migration of ECs, we have reported a strategy for biodegradable microparticles complexed with pEGFP-ZNF580 (pZNF580) gene to regulate the endothelialization of ECs.[25,26] Actually, as an effective gene carrier, it is essential that the gene carrier could be uptaken specifically by ECs in the complex bloodstream environment *in vivo*. More precisely, a well-designed gene carrier for actively targeting ECs should be swallowed only by ECs over other cells, especially human artery smooth muscle cells (SMCs). Therefore, it is of great interest to investigate whether it is possible to develop actively targeting nanoparticles condensed with genes to realize the specific adhesion and proliferation of ECs.

Recently, many strategies have been explored to prepare gene carriers with targeting function. For example, Wang and his co-workers investigated the targeting iron-oxide nanoparticle for photodynamic therapy and imaging of head and neck cancer.[27] Kang and his co-workers reported on liver-targeting siRNA delivery based on PEI-pullulan carrier.[28] Lee prepared a cysteamine modified gold NPs/siRNA/PEI/hyaluronic acid complex using a layer-by-layer method.[29] Moreover, Gu and his co-workers prepared dual-functional liposomes with mitochondria and pH response to overcome drug-resistant lung cancer.[30] In treatment of glioblastoma *in vivo*, gold nanorods/PEG−PCL hybrid nanoparticles with a cRGD-directed process, NIR-responsiveness, and robustness were reported for targeted chemotherapy by Zhong and his co-workers.[31] Jiang developed casoactive peptide-decorated chitosan nanoparticles for enhancing drug accumulation and penetration in a subcutaneous tumor.[32] Although various targeting gene carriers have been widely studied in the treatment of different cancers,[33] gene carriers for actively targeting ECs have been rarely reported.[34,35] Therefore, it is very important to design and study actively targeting gene carriers which can be selected specifically by ECs and to enhance endothelialization.

To this end, with great interest, the NPs were designed and synthesized for actively targeting ECs using biodegradable copolymers and REDV peptide. We synthesized series of REDV peptide modified block copolymers, namely, REDV-*g*-polyethylenimine-*g*-poly(lactide-*co*-glycolide)-*g*-polyethylenimine-*g*-REDV (REDV-*g*-PEI-*g*-P(LA-*co*-GA)-*g*-PEI-*g*-REDV) and REDV-*g*-polyethylenimine-*g*-poly(lactide-*co*-glycolide-*co*-3(S)-methyl-morpholine-2,5-dione)-*g*-polyethylenimine-*g*-REDV (REDV-*g*-PEI-*g*-P(LA-*co*-GA-*co*-MMD)-*g*-PEI-*g*-REDV). And then, by nanoprecipitation technology, we prepared actively targeting NPs for ECs from biodegradable block copolymers having REDV functional peptides, which were then condensed with pZNF580 to generate NPs/pZNF580 complexes. The properties of the copolymers, NPs, and NPs/pZNF580 complexes were investigated. The REDV peptide conjugated NPs/pZNF580 complexes showed low cytotoxicity and excellent active targeting function for ECs.

2. MATERIALS AND METHODS

2.1. Materials. Polyethylenimine (branched PEI, M_w = 1800), 1,8-octanediol, 3-(4,5-dimethylthiazol-2-yl)-2,5-diphenyltetrazolium bromide (MTT), 2,2-dimethoxy-2-phenylacetophenone (DMPA), 4′,6-diamidino-2-phenylindole (DAPI), fluorescein isothiocyanate (FITC), rhodamine B isothiocyanate (RBITC), FITC labeled CD31, RBITC labeled α-SMA and *N*,*N*-dimethylformamide (DMF), dibutyl tin dilaurate (DBTDL), and stannous octoate ($Sn(Oct)_2$) were purchased from Sigma-Aldrich (St. Louis, MO). L-Lactide (L-LA) and glycolide (GA) were obtained from Foryou Medical Device Co., Ltd. (Huizhou, China). L-Alanine and chloroacetyl chloride were supplied by Aladdin Reagent Co., Ltd. (Shanghai, China). Dimethyl sulfoxide (DMSO) was purchased from Sigma (St. Louis, MO). CREDVW peptide was purchased from GL Biochem (Shanghai) Ltd. (Shanghai, China). Lipofectamine 2000 reagent was purchased from Invitrogen (Grand Island, NY). pZNF580 was preserved by the Department of Physiology and Pathophysiology, Logistics University of Chinese People's Armed Police Force. 3(*S*)-Methyl-morpholine-2,5-dione (MMD) monomer was prepared using our previously reported method.[26]

2.2. Synthesis of Amphiphilic Triblock Copolymers.

2.2.1. Synthesis of P(LA-co-GA) and P(LA-co-GA-co-MMD) Copolymers. P(LA-*co*-GA) copolymer was prepared as reported previously by ring-opening polymerization (ROP). Briefly, 1,8-octanediol, LA, GA, and $Sn(Oct)_2$ toluene solution (2.9 wt %) were added in a flame-dried and nitrogen-purged flask (10 mL). The flask was sealed and maintained at 120 °C for 12 h. The copolymer was recovered by dissolution in chloroform and followed by precipitation in hexane. This process was performed 3 times to obtain purified copolymers. The resultant precipitate (P(LA-*co*-GA) copolymer) was filtered and dried at room temperature in vacuum until it reached a constant weight. Moreover, P(LA-*co*-GA-*co*-MMD) copolymer was synthesized using a similar method.

2.2.2. Synthesis of Triblock Copolymers. PEI-*g*-P(LA-*co*-GA)-*g*-PEI triblock copolymer was synthesized after graft PEI from P(LA-*co*-GA) copolymers. Copolymer (1.0 g) was dissolved in anhydrous chloroform (9.5 mL), and then the solution was transferred into a dried constant pressure funnel (25 mL). DBTDL (10 μL) and isophorone diisocyanate (IPDI) toluene solution (638 μL, 1 wt %) were added in a three-necked flask (50 mL). P(LA-*co*-GA) copolymer solution was added dropwise with stirring at 30 °C in 30 min, and it then reacted for 24 h. The reaction mixture was added dropwise into 5.24 mL of PEI toluene solution (10 wt %) stirred at a suitable speed (1000 rpm) under a nitrogen atmosphere at 60 °C in 3 h, and then reacted for 24 h. When the solution was cooled to room temperature, triblock copolymer of (PEI-*g*-P(LA-*co*-GA)-*g*-PEI) was obtained by precipitation in ice-cold hexane as white flocculent precipitate. The copolymer was dissolved in chloroform and precipitated with anhydrous ether, and the process was performed 3 times to obtain purified triblock copolymer. The resultant precipitate was filtered and dried at room temperature in vacuum until it reached a constant weight. The triblock copolymer of PEI-*g*-P(LA-*co*-GA-*co*-MMD)-*g*-PEI was synthesized using a similar method.

2.2.3. Graft of REDV Peptide. REDV peptide grafted triblock copolymer of PEI-*g*-P(LA-*co*-GA)-*g*-PEI was prepared by two steps. First, in order to introduce the carbon−carbon double bond, some amino groups ($-NH_2$) of the PEI-*g*-P(LA-*co*-GA)-*g*-PEI copolymers reacted with diallylcarbamic acid chloride as reported previously.[36] Second, CREDVW peptides were grafted by "Michael addition reaction" as reported before.[37]

Briefly, PEI-*g*-P(LA-*co*-GA)-*g*-PEI copolymer (0.50 g) was dissolved in DMF (5.0 mL). Then, the polymer solution was transferred to a flask (50 mL), and 39 μL triethylamine was added into the solution. A 5.0 mL portion of diallylcarbamic chloride DMF solution (0.9 wt %) was added dropwise to the solution with continuous stirring at 0 °C. The reaction was maintained at room temperature for 12 h. Then, the solution was filtered with sand core funnel, and the filtrate was transferred to a Petri dish. A 5.0 mg portion of DMPA was added into the solution. A 2.0 mL portion of CREDVW DMF solution (containing 300 mg CREDVW peptide) was added to the solution. Then, the solution was irradiated under the ultraviolet light (365 nm UV-lamp) using DMPA as photoinitiator for 10 min to complete the reaction.[38] Copolymer was recovered by precipitation in ice-cold hexane, then dissolved in DMF, and precipitated in ice-cold hexane; the process was performed for 3 times to remove the unreacted residues. The resultant precipitate was filtered and dried at room temperature in vacuum until it reached a constant weight. Finally, the copolymers named REDV-*g*-PEI-*g*-P(LA-*co*-GA)-*g*-PEI-*g*-REDV were

DOI: 10.1021/acsami.5b06286
ACS Appl. Mater. Interfaces 2015, 7, 20389−20399

obtained. REDV peptide grafted triblock copolymer of REDV-*g*-PEI-*g*-P(LA-*co*-GA-*co*-MMD)-*g*-PEI-*g*-REDV was also synthesized using a similar method.

2.3. Characterization of Copolymers. ^{1}H NMR spectra of the synthesized polymers were recorded with a Bruker Avance spectrometer (AV-400, Bruker, Karlsruche, Germany) operating at 400 MHz in $CDCl_3$ or DMSO-d_6. FT-IR spectra of the copolymers were obtained using a FT-IR spectrometer (Bio-Rad FTS-6000, MA). Moreover, the average molecular weight (M_n) was determined by gel permeation chromatography (GPC, Malvern Viscotek, U.K.) with GPCmax 270 column in tetrahydrofuran (THF). The standard polymers were Shodex STANDARD SM-105 (Lot No. 10203).

2.4. Degradation of the Copolymers *in Vitro*. Biodegradation test was employed as reported previously to study the degradation behavior of the copolymers *in vitro*.[25,39] The residual weight (%) of the copolymers was calculated using the following formula (W_0, the original weight of the copolymer sample; W_t, the sample weight at different time interval):

$$\text{residual weight (\%)} = \frac{W_t}{W_0} \times 100\%$$

2.5. Preparation and Characterization of NPs/pZNF580 Complexes. *2.5.1. Preparation of NPs.* NPs were prepared using nanoprecipitation technology. Briefly, 10.0 mg of amphiphilic triblock copolymer was dissolved in 1 mL of THF. The solution was added dropwise to 10 mL of triple-distilled water stirred at reasonable speed (400−1500 rpm) in a beaker in 1 h. Then, to remove THF, the mixture solution was stirred at room temperature for 24 h in a fume cupboard. For further experiments, the final volume of the solution was adjusted to 10 mL.

2.5.2. Preparation of NPs/pZNF580 Complexes. The suspension of pZNF580 was diluted to 1 μg/50 μL with PBS buffer (pH = 7.4). The complexes were prepared by adding NP suspension (1 mg/mL) to pZNF580 suspension (containing 1 μg) at various N/P molar ratios (0.5:1, 1:1, 2:1, 5:1, 10:1, and 20:1). Before characterization and further experiments, the complexes were mixed gently and incubated for 30 min at room temperature in a clean bench. N/P molar ratios were calculated from weight of polymer and plasmid, N content in the polymer and P content in plasmid.

2.5.3. Size Distribution and Zeta Potential. The size and zeta potential of NPs and NPs/pZNF580 complexes were measured using a Zetasizer 3000HS (Malvern Instrument, Inc., Worcestershire, U.K.) as reported previously at the wavelength of 677 nm with a constant angle of 90°.[26]

2.5.4. Agarose Gel Electrophoresis. Agarose gel electrophoresis was employed as reported previously to assess the DNA condensation ability of NPs.[26] The NPs/pZNF580 complexes with various N/P molar ratios ranging from 0.5 to 20 were prepared. The mixture solution was loaded into the agarose gel (0.8 wt %) containing 0.5 μg/mL ethidium bromide. Electrophoresis was performed in 1× TAE buffer at 100 V for 40 min; UV illuminator was used to indicate the retarded location of the plasmids.

2.5.5. In Vitro Release of pZNF580. To assess the pZNF580 release ability from the NPs/pZNF580 complexes, release assay *in vitro* was employed as reported previously.[25] By measuring the extinction fluorescence with ethidium bromide, the adsorption efficiency of plasmid DNA was obtained. The supernatant was analyzed using Cary Eclipse fluorescence spectrometer at excitation wavelength of 524 nm and emission wavelength of 582 nm.[40]

2.5.6. Morphology of NPs and NPs/pZNF580 Complexes. The morphological study of NPs and NPs/pZNF580 complexes was performed on JME100CXII transmission electron microscope (TEM, JEOL Ltd. Japan). Samples were prepared using the method reported previously.[41] Briefly, NP suspension (1 mg/mL) and NPs/pZNF580 suspensions were dipped onto a carbon-coated copper grid. Then, the carbon-coated copper grid dried in the air for 10 h before images were taken.

2.6. Transfection and Cytotoxicity. *2.6.1. Cell Culture.* ECs and SMCs were purchased from American Type Culture Collection, and were cultured in high glucose DMEM supplemented 10% FBS in 5% CO_2 atmosphere at 37 °C. The next day, the nonadherent cells were discarded, and the adherent cells were cultured to confluence with medium exchanges being conducted every 3 days.

2.6.2. Transfection of NPs/pZNF580 Complexes in Vitro. ECs were transfected using the same method as reported previously.[25] The expression of green fluorescence protein (GFP) in cells was observed under an inverted fluorescent microscope at different time intervals.

2.6.3. Protein Extraction and Western Blotting Analysis. Western blot analysis was performed as reported previously.[25,42] Proteins were incubated with horseradish peroxidase conjugated to goat antirabbit Ig G to assess the protein loading level, and then they were incubated with enhanced chemiluminescence reagent and were exposed to film. The belt was analyzed using ImageJ 2.1, and β-actin antibody was used as a control.

2.6.4. In Vitro Cytotoxicity of NPs and NPs/pZNF580 Complexes. The cytotoxicity of NPs and NPs/pZNF580 complexes was evaluated by MTT assay using PEI (M_w = 10 000) as the control group, and the relative cell viability was calculated finally.[25] Optical density (OD) was measured by an ELISA reader (Titertek multiscan MC) at the wavelength of 490 nm. The relative cell viability (%) was calculated using the following formula: (OD490′, the absorbance value of experimental wells minus zero wells; avg(OD490C′), the average absorbance value of corrected control wells).

$$\text{relative cell viability} = \frac{\text{OD490}'}{\text{avg(OD490C}')} \times 100\%$$

2.6.5. Wound Healing Assay of ECs. The migration ability of ECs transfected by NPs/pZNF580 complexes was assessed using a scratch wound healing assay.[25,43] The migration process at different time points was monitored using an inverted microscope; the migration area was calculated using ImageJ 2.1 based on the images after 12 h. The measure of the wounded area was calculated by the following formula: wounded area = length × width. The percentage of migration area was calculated by the following formula: relative recovered surface area (%) = (wounded area − nonrecovered area)/wounded area.[44]

2.6.6. Migration Assay of ECs. Assessment of endothelial cell migration was performed using a transwell assay.[45] The upper surface of polycarbonate filters with 8-μm pores was put with DMEM and cultured for 30 min. Cells treated with different NPs/pZNF580 complexes. Then, cells were extensively washed with DMEM containing 1% acid-free bovine serum albumin and resuspended in the same medium. DMEM in the presence of 10% FBS was loaded in the lower chambers as a chemotaxis inducer. Cells (1×10^4 cells/mL at 200 μL per well) were plated in the upper chambers and allowed to migrate through the 8-μm porous filters at 37 °C for 6 h. Nonmigrating cells on the upper surface of the filter were wiped off with a cotton swab. Migrating cells which adhered to the lower surface were stained with eosin, and observed using optical microscope.

2.7. Actively Targeting Ability of NPs/pZNF580 Complexes. ECs and SMCs (1:1) were added to the culture flask with 5 mL of DMEM medium (10% FBS). Then, the cells were mixed gently and incubated for 2−3 days until 80−90% confluence. Cells were trypsinized using 0.25% trypsin. After resuspension, cells were cultured with different NPs/pZNF580 complexes for another 24 h. Then, cells were fixed using 4% paraformaldehyde, and treated with 0.5% Triton X-100 to improve the permeability of the cell membrane. Finally, cells were dyed using different dyes (DAPI, FITC, and RBITC).[46]

2.8. Statistical Analysis. All experiments were performed at least three times. Quantitative data are presented as the mean ± SD. Statistical comparisons were made with Student's *t* test. *P*-values (<0.05) were considered to be statistically significant.

3. RESULTS

3.1. Synthesis of Amphiphilic Block Copolymers. Amphiphilic block copolymers were prepared by ROP and grafting reaction. We take REDV-*g*-PEI-*g*-P(LA-*co*-GA-*co*-MMD)-*g*-PEI-*g*-REDV copolymer as an example (the synthesis

DOI: 10.1021/acsami.5b06286
ACS Appl. Mater. Interfaces 2015, 7, 20389−20399

route is shown in Scheme S1 (Supporting Information)). Herein, 1,8-octanediol was used as the initiator to control the molecular weight of P(LA-*co*-GA) and P(LA-*co*-GA-*co*-MMD) copolymers. The amphiphilic triblock copolymers were prepared by grafting PEI. The yield percent values of the P(LA-*co*-GA) and P(LA-*co*-GA-*co*-MMD) ranged from 75% to 80%. But yield of the PEI-*g*-P(LA-*co*-GA)-*g*-PEI and PEI-*g*-P(LA-*co*-GA-*co*-MMD)-*g*-PEI ranged from 50% to 60%.

In order to endow NPs with active targeting for ECs, REDV peptides were linked onto PEI chains. Then, molecular weight of the block copolymers was estimated by ^{1}H NMR and determined by GPC. The content of PEI, LA, GA, and MMD in the block copolymers was estimated by ^{1}H NMR (Table S1). The yield of peptide-grafted triblock copolymers ranged from 60% to 70%.

The copolymers were characterized by FT-IR and shown in Figure 1. The stretching frequency of the secondary amide

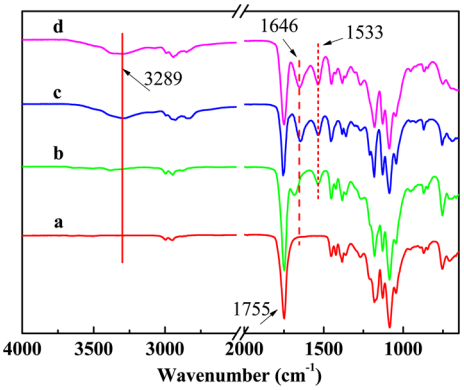

Figure 1. FT-IR spectra of copolymers: (a) copolymer of P(LA-*co*-GA)$_1$, (b) copolymer of P(LA-*co*-GA-MMD)$_1$, (c) triblock copolymer PEI-*g*-P(LA-*co*-GA)-*g*-PEI$_1$, and (d) triblock copolymer PEI-*g*-P(LA-*co*-GA-*co*-MMD)-*g*-PEI$_1$.

(−CO−NH−) in an MMD segment was found at 3289 cm^{-1} (−NH−), 1687 cm^{-1} (amide I), and 1533 cm^{-1} (amide II) (Figure 1b); the signal at 1755 cm^{-1} was assigned to the carboxylate group (−O−CO−) in P(LA-*co*-GA)$_1$ and P(LA-*co*-GA-MMD)$_1$ copolymers.[47] After a graft of PEI, the symmetric stretching characteristic peaks of primary amine (−NH$_2$) were found at 3289 and 1646 cm^{-1}.[48] These results indicated that triblock copolymers were synthesized successfully.

The copolymers were characterized by ^{1}H NMR (Figure S1). ^{1}H NMR spectrum of P(LA-*co*-GA)$_1$ copolymer in $CDCl_3$ showed that there are peaks at δ 5.19 ppm (−COC**H**(CH_3)O−, 1H), δ 4.82 ppm (−COC**H**$_2$O-, 2H), and δ 1.59 ppm (−COCH(C**H**$_3$)O−, 3H).[49] ^{1}H NMR spectrum of PEI-*g*-P(LA-*co*-GA)-*g*-PEI$_1$ tribolck copolymer in DMSO-d_6 exhibited the characteristic peak of the protons of PEI at δ 2.4−3.2 ppm.[50] These results confirmed that the PEI-*g*-P(LA-*co*-GA)-*g*-PEI$_1$ triblock copolymer was synthesized perfectly.

In order to endow NPs with active targeting selectivity for ECs, CREDVW peptide was grafted onto PEI chains (Figure 2). Herein, the sequence of the peptide was designed as CREDVW. Owing to the mercapto group (−SH), cysteine residue in CREDVW peptide was linked onto diallylcarbamic PEI by Michael addition reaction. CREDVW peptide can be detected and calculated by the fluorescence intensity of indole in tryptophan residue (Figure S2). The CREDVW modified amphiphilic block copolymers showed obvious absorption peak at 362 nm.

3.2. Degradation Behavior of Copolymers. The degradation behavior of triblock copolymers was investigated *in vitro* (Figure 3). After 50 days, the residual weight of PEI-*g*-P(LA-*co*-GA)-*g*-PEI$_1$ copolymer decreased to 75.0%. PEI-*g*-P(LA-*co*-GA-*co*-MMD)-*g*-PEI$_1$ copolymer showed a faster weight loss than PEI-*g*-P(LA-*co*-GA)-*g*-PEI$_1$ copolymer, and the residual weight was only 50.6%.

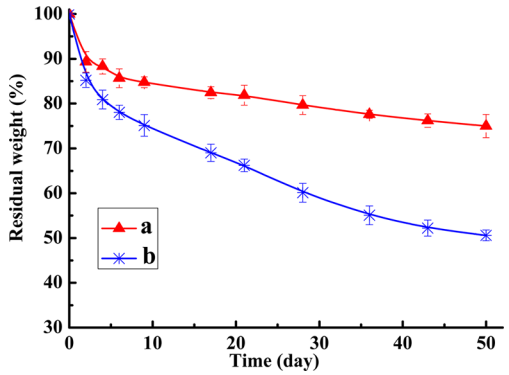

Figure 3. Residual weight of the copolymers in PBS (pH = 7.4), at 37 °C, under constant shaking (30 rpm): (a) PEI-*g*-P(LA-*co*-GA)-*g*-PEI$_1$ triblock copolymer, (b) PEI-*g*-P(LA-*co*-GA-*co*-MMD)-*g*-PEI$_1$ triblock copolymer. Error bars represent the standard deviations (n = 3).

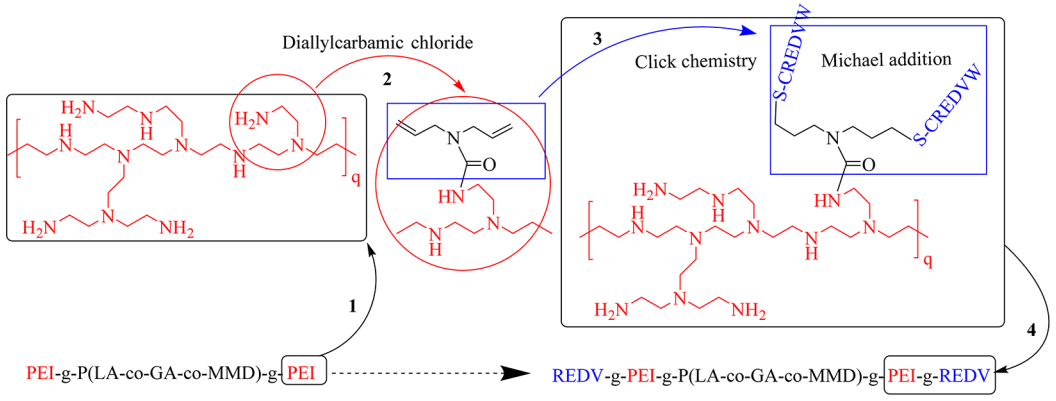

Figure 2. Grafting route of CREDVW peptide onto the triblock copolymer.

DOI: 10.1021/acsami.5b06286
ACS Appl. Mater. Interfaces 2015, 7, 20389−20399

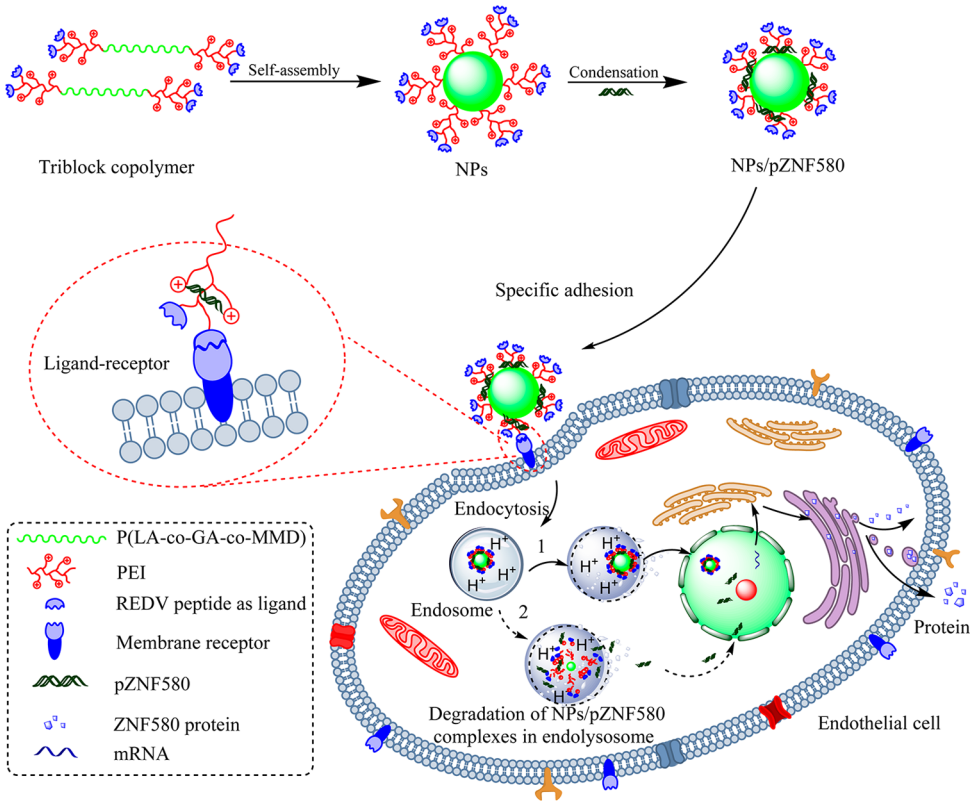

Figure 4. Self-assembly of the NPs from amphiphilic triblock copolymers and the process of active targeting adsorption mediated by targeting NPs/pZNF580 complexes. NPs were prepared by self-assembly, and NPs/pZNF580 complexes were formed by condensation with pZNF580. As the active targeting ligand, REDV peptide on the surface can be recognized and bound specifically by the surface receptor. The complex was transfected into the cell via endocytosis; through path 1 or 2, the plasmids entered into the cell nucleus.

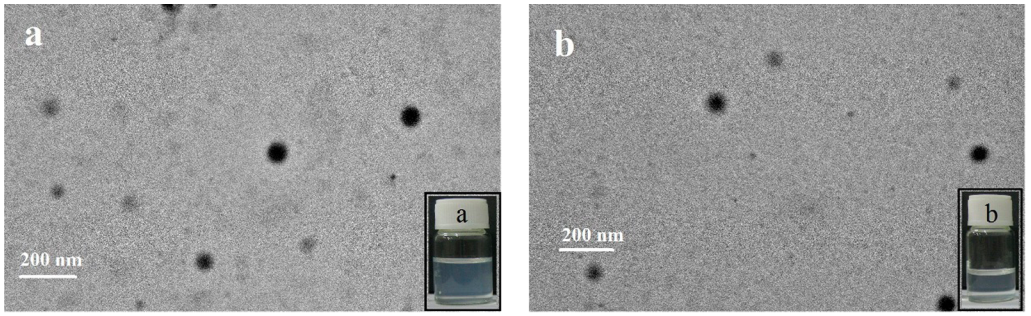

Figure 5. TEM images of NPs and NPs/pZNF580 complexes: (a) NPs prepared from REDV-*g*-PEI-*g*-P(LA-*co*-GA)-*g*-PEI-*g*-REDV$_1$ triblock copolymer, (b) NPs/pZNF580 complexes (N/P = 5) prepared from REDV-*g*-PEI-*g*-P(LA-*co*-GA)-*g*-PEI-*g*-REDV$_1$ based NPs and pZNF580.

The degradation process of triblock copolymers had two stages. The residual weight of all copolymers decreased quickly during the initial 5 days in the first stage. In this stage, the residual weight of all copolymers decreased quickly, which is due to the hydrolysis of the ester bonds in the hydrophobic segments (P(LA-*co*-GA-*co*-MMD) and P(LA-*co*-GA)) nearly connected with the hydrophilic chains of PEI. Therefore, PEI segments dissolved quickly along with the degradation of the ester bonds in PBS.

In the second stage, PEI-*g*-P(LA-*co*-GA-*co*-MMD)-*g*-PEI$_1$ copolymer showed a faster degradation rate than PEI-*g*-P(LA-*co*-GA)-*g*-PEI$_1$ copolymer. When MMD copolymerized with LA and GA to form the random copolymer of P(LA-*co*-GA-*co*-MMD), the chain of this copolymer had random amide and ester groups. The amide groups increased the hydrophilicity of copolymer chains, which resulted in high water absorption during the second degradation stage. This is the main reason that leads to a high degradation rate for PEI-*g*-P(LA-*co*-GA-*co*-MMD)-*g*-PEI$_1$ copolymer.[51]

3.3. Morphology of NPs and NPs/pZNF580 Complexes. In aqueous solution, amphiphilic triblock copolymers can assemble into NPs with core−shell structure (Figure 4). The hydrophobic segments, such as P(LA-*co*-GA) or P(LA-*co*-GA-*co*-MMD), formed the core of NPs, while PEI and REDV peptide as the hydrophilic segments preferred existing in the hydrophilic shell surrounding the core.

When NPs/pZNF580 complexes were cultured with cells in the medium, owing to the actively targeting ligands (REDV peptides) on their surface, these complexes can be recognized and adhered specifically by the membrane receptor ($\alpha_4\beta_1$ integrin), and then entered efficiently into ECs by cytophagy (Figure 4). After escape from endolysosome, NPs/pZNF580

DOI: 10.1021/acsami.5b06286
ACS Appl. Mater. Interfaces 2015, 7, 20389−20399

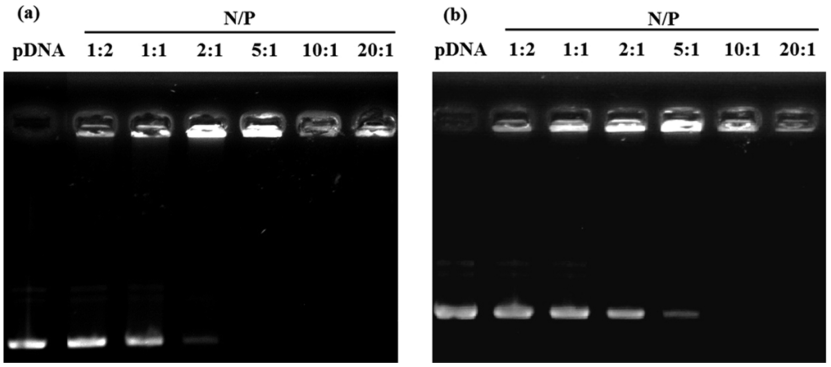

Figure 6. Agarose gel electrophoresis of NPs/pZNF580 complexes at various N/P molar ratios: (a) REDV-*g*-PEI-*g*-P(LA-*co*-GA)-*g*-PEI-*g*-REDV$_1$ based NPs/pZNF580 complexes and (b) REDV-*g*-PEI-*g*-P(LA-*co*-GA-*co*-MMD)-*g*-PEI-*g*-REDV$_1$ based NPs/pZNF580 complexes.

complexes or plasmids could enter into the cell nucleus through path 1 or 2 (Figure 4).[52] This process of endocytosis and intracellular trafficking has been confirmed by Cameron and co-workers.[53] As the key protein to promote the proliferation of ECs, the overexpression of ZNF580 protein will promote the proliferation and migration of ECs.

3.4. Size and Zeta Potential. The hydrodynamic diameter and zeta potential of NPs were measured by a Zetasizer 3000HS and summarized in Table S2. The size of NPs ranged from 66.3 ± 10.5 nm to 75.1 ± 6.1 nm with a reasonable polydispersity index (PDI < 0.3); the zeta potential ranged from 24.1 ± 0.9 mV to 31.6 ± 0.6 mV. In the following study, REDV-*g*-PEI-*g*-P(LA-*co*-GA)-*g*-PEI-*g*-REDV$_1$ and REDV-*g*-PEI-*g*-P(LA-*co*-GA-*co*-MMD)-*g*-PEI-*g*-REDV$_1$ based NPs were selected due to their reasonable size and appropriate positive potential.

At room temperature, by mixing the NP suspension with pZNF580 solution in PBS (pH = 7.4), NPs/pZNF580 complexes were prepared and allowed for 30 min to form NPs/pZNF580 complexes. As shown in Figure 5, the morphology of NPs and NPs/pZNF580 complexes (N/P = 5) exhibited a spherical structure. However, the nanoparticle size (about 60 nm) measured by TEM was smaller than those obtained by a nanoparticle size and zeta potential analyzer. The reason is attributed to the hydrodynamic size measured by nanoparticle size and zeta potential analyzer in the hydrated state in solution, while TEM showed the size of dried NPs on carbon-coated copper meshes.

For well-designed gene carriers, it is of great importance that there is effective condensation of negatively charged pZNF580 through electrostatic interaction.[54] Therefore, a gel retardation assay was employed to verify the successful binding ability between NPs and pZNF580. As we know, NPs with or without pZNF580 are too large to diffuse through the agarose matrix. Therefore, only the plasmids which are not bound by NPs can migrate to the positive electrode as the naked plasmids.[55] Before the gel retardation assay, NPs/pZNF580 complexes with different N/P molar ratios were incubated at room temperature for 30 min. The images of gel retardation assay were shown in Figure 6. When the N/P molar ratio rose to 5, the plasmids were almost bound by the two kinds of NPs. These results demonstrated that the two kinds of NPs exhibited effective binding ability, because these NPs had very high zeta potential, namely, 31.6 ± 0.6 and 29.3 ± 1.2 mV, respectively (Table S2). Therefore, the NPs prepared in the present study exhibited effective binding ability to plasmids.

3.5. *In Vitro* Release of pZNF580. During gene clinic therapy, it is an important property for gene carriers to exhibit an ideal sequential gene release.[56] Therefore, to investigate the characteristic of plasmid release from NPs/pZNF580 complexes, the release assay was carried out in Tris-HCl buffer (pH = 7.4) at 37 °C *in vitro* (Figure S3). During the initial 6 days, all of the complexes showed a rapid nucleic acid release behavior. However, after 28 days, the cumulative release of the plasmids from the complexes at N/P ratio of 5 was higher than that at N/P ratio of 20. When the N/P ratio was raised to 20, the electrostatic interaction between NPs and plasmids was very strong. Therefore, high electrostatic binding force prevented the rapid release of plasmids from the complexes.

In addition, in accounting for the release of plasmids, another main reason which could not be ignored is that there are different degradation rates of the copolymers. The degradation rate of PEI-*g*-P(LA-*co*-GA-*co*-MMD)-*g*-PEI copolymer was faster than the others (Figure 3). Therefore, at the N/P molar ratio of 5, the cumulative release of plasmids (87.7%, Figure S3b) from REDV-*g*-PEI-*g*-P(LA-*co*-GA-*co*-MMD)-*g*-PEI-*g*-REDV$_1$ based NPs/pZNF580 complexes was higher than that from REDV-*g*-PEI-*g*-P(LA-*co*-GA)-*g*-PEI-*g*-REDV$_1$ based complexes (75.6%, Figure S3a).

3.6. *In Vitro* Transfection. The expression of green fluorescence protein was used to qualitatively determine whether the plasmids had been transfected into ECs. Therefore, GFP was observed under an inverted fluorescent microscope. After 48 h of transfection, many cells with green fluorescence could be observed (Figure 7 b–d). These results demonstrated that the plasmids had been carried into cells by NPs/pZNF580 complexes, and then the GFP gene had expressed successfully in these cells.

Western blot detection was employed to quantitatively characterize the expression of ZNF580 gene in ECs. The relative protein level of cells treated with REDV-*g*-PEI-*g*-P(LA-*co*-GA-*co*-MMD)-*g*-PEI-*g*-REDV$_1$ based NPs/pZNF580 complexes reached 34.8% (Figure 8 b), while that of cells treated with REDV-*g*-PEI-*g*-P(LA-*co*-GA)-*g*-PEI-*g*-REDV$_1$ based NPs/pZNF580 complexes was only 21.3% (Figure 8 c). However, the relative protein level of cells treated with Lipofectamine TM 2000 (the positive control group) was 33.2%, which has been reported in our previous research.[25] The rapid degradation of PEI-*g*-P(LA-*co*-GA-*co*-MMD)-*g*-PEI$_1$ triblock copolymer (Figure 3 b) provided a fast release of pZNF580. This might be the main reason for the overexpression of ZNF580 gene in the cells treated with REDV-*g*-PEI-*g*-P(LA-*co*-GA-*co*-MMD)-*g*-PEI-*g*-REDV$_1$ based NPs/pZNF580 complexes.

DOI: 10.1021/acsami.5b06286
ACS Appl. Mater. Interfaces 2015, 7, 20389–20399

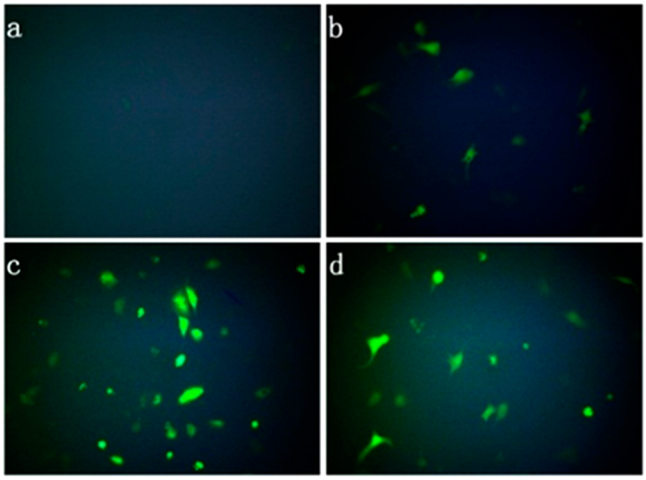

Figure 7. Fluorescence images of ECs transfected by different NPs/pZNF580 complexes (N/P = 5) at concentration of 80 μg/mL and Lipofectamine 2000 group: (a) cells treated with neither any complexes nor the Lipofectamine 2000 group, which served as the negative control group, (b) cells treated with REDV-*g*-PEI-*g*-P(LA-*co*-GA)-*g*-PEI-*g*-REDV$_1$ based NPs/pZNF580 complexes (N/P = 5), (c) cells treated with REDV-*g*-PEI-*g*-P(LA-*co*-GA-*co*-MMD)-*g*-PEI-*g*-REDV$_1$ based NPs/pZNF580 complexes (N/P = 5), and (d) cells treated with Lipofectamine 2000 group (N/P = 5) which served as the positive control group.

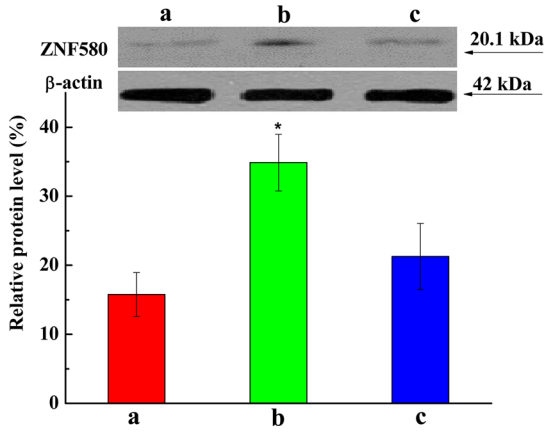

Figure 8. Western blot analysis for ZNF580 protein expression after 48 h ($\bar{x}$ + SD, n = 3, *p < 0.05 vs a group): (a) cells treated with neither any complexes nor with Lipofectamine 2000 group served as the negative control group, (b) cells treated with REDV-*g*-PEI-*g*-P(LA-*co*-GA-*co*-MMD)-*g*-PEI-*g*-REDV$_1$ based NPs/pZNF580 complexes (N/P = 5), and (c) cells treated with REDV-*g*-PEI-*g*-P(LA-*co*-GA)-*g*-PEI-*g*-REDV$_1$ based NPs/pZNF580 complexes (N/P = 5).

3.7. *In Vitro* Cytotoxicity. For PEI based gene carriers, the cytotoxicity is a serious issue. Herein, an MTT assay was employed to evaluate the toxicity of the prepared NPs and NPs/pZNF580 complexes (Figure 9). The relative cell viability of NPs and their NPs/pZNF580 complexes was much higher than that of PEI at the same concentration. Furthermore, the relative cell viability of their NPs/pZNF580 complexes was relatively higher than that of their NPs.

Even at the high concentration (100 μg/mL), NPs/pZNF580 complexes only showed mild cytotoxicity (relative cell viability >80%). This phenomenon can be explained by the neutralization between positive and negative charges.[57] When the plasmids were adsorbed to the surface of NPs, the positive

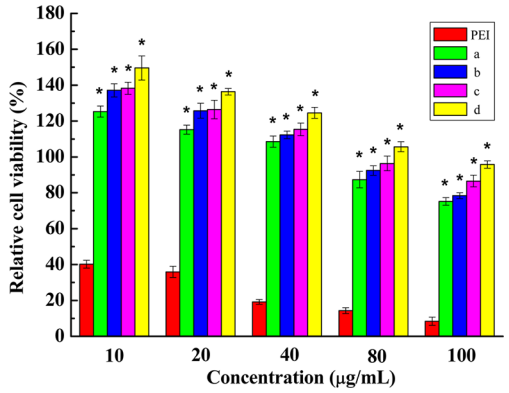

Figure 9. Relative cell viability after 48 h of treatment with different concentrations of NPs and NPs/pZNF580 complexes at N/P molar ratio of 5. Cells treated with PEI (M_w = 10 000) served as the control group. (a) Cells treated with REDV-*g*-PEI-*g*-P(LA-*co*-GA)-*g*-PEI-*g*-REDV$_1$ based NPs. (b) Cells treated with REDV-*g*-PEI-*g*-P(LA-*co*-GA-*co*-MMD)-*g*-PEI-*g*-REDV$_1$ based NPs. (c) Cells treated with REDV-*g*-PEI-*g*-P(LA-*co*-GA)-*g*-PEI-*g*-REDV$_1$ based NPs/pZNF580 complexes. (d) Cells treated with REDV-*g*-PEI-*g*-P(LA-*co*-GA-*co*-MMD)-*g*-PEI-*g*-REDV$_1$ based NPs/pZNF580 complexes ($\bar{x}$ + SD, n = 6, *p < 0.05 vs PEI group).

charges of PEI were partly neutralized by the negative charges of plasmids, which minimized direct contact of the positive charge with the cell membrane.

At low concentration (40 μg/mL), NPs and their complexes exhibited almost noncytotoxicity. At this concentration, the proliferations of ECs were promoted obviously. The main reason was that the degradation product, such as L-alanine, released from the hydrophobic core, might stimulate the proliferation of ECs via a signal pathway.[58] These results manifested that these biodegradable NPs should be a suitable gene carrier with noncytotoxicity.

3.8. Migration of ECs Treated with NPs/pZNF580 Complexes. During the wound healing process, cell migration and proliferation play a vital role. Therefore, the scratch assay was usually used to study the proliferation and migration properties of cells. ECs were transfected with NPs/pZNF580 complexes at the N/P molar ratio of 10. After 48 h, a monolayer of ECs was formed in a 6-well plate. An artificial scratch with parallel borders was mechanically created (Figure S4A(a)). Then, at different time intervals, the time course of the migration process to close this "wound" scratch was monitored using an inverted microscope (Figure S4A(b) and (c)). The relative recovered surface area was calculated by Image-Pro Plus (6.0).

After 12 h, the relative recovered surface area of cells transfected by REDV-*g*-PEI-*g*-P(LA-*co*-GA)-*g*-PEI-*g*-REDV$_1$ based NPs/pZNF580 complexes increased to 81.3 ± 6.8% (Figure S4B(2)). Furthermore, the cells transfected by REDV-*g*-PEI-*g*-P(LA-*co*-GA-*co*-MMD)-*g*-PEI-*g*-REDV$_1$ based NPs/pZNF580 complexes migrated to cover 94.6 ± 7.3% of the scratch area (Figure S4B(3)). Due to the different degradation speed during the cell culture process (Figure 3), the relative recovered surface area of cells transfected with REDV-*g*-PEI-*g*-P(LA-*co*-GA-*co*-MMD)-*g*-PEI-*g*-REDV$_1$ based NPs/pZNF580 complexes was much larger than that transfected with REDV-*g*-PEI-*g*-P(LA-*co*-GA)-*g*-PEI-*g*-REDV$_1$ based NPs/pZNF580 complexes. These results suggested that, after 60 h (transfection 48 h before scratching plus 12 h after scratching), the migration

DOI: 10.1021/acsami.5b06286
ACS Appl. Mater. Interfaces 2015, 7, 20389−20399

of ECs was promoted greatly by ZNF580 gene released from NPs/pZNF580 complexes.

Transwell assay was designed to investigate the migration ability of ECs treated with different NPs/pZNF580 complexes. Cells not treated as the negative control group exhibited poor migration ability (Figure 10a). However, it was obviously

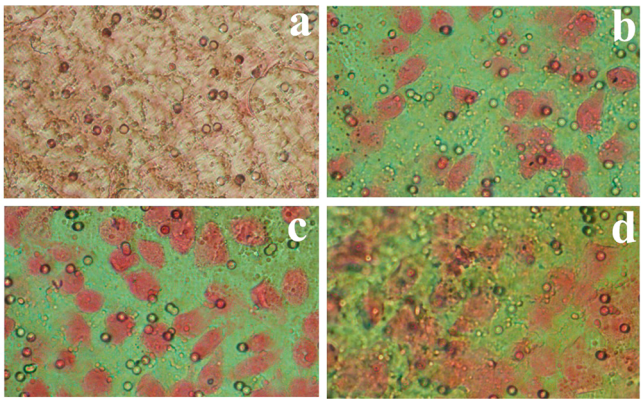

Figure 10. Results of transwell assay: (a) cells treated with neither NPs/pZNF580 complexes nor the Lipofectamine 2000 group served as the negative control group, (b) cells treated with REDV-*g*-PEI-*g*-P(LA-*co*-GA)-*g*-PEI-*g*-$REDV_1$ based NPs/pZNF580 complexes, (c) cells treated with REDV-*g*-PEI-*g*-P(LA-*co*-GA-*co*-MMD)-*g*-PEI-*g*-$REDV_1$ based NPs/pZNF580 complexes, (d) cells treated with Lipofectamine 2000 group served as the positive control group.

observed that a large number of ECs treated with NPs/pZNF580 complexes were dyed into red by eosin (Figure 10b,c). Compared with the negative control group, the cells transfected with NPs/pZNF580 complexes showed significant migration ability, which was almost similar to the Lipofectamine 2000 group (the positive control group, Figure 10d). Therefore, the NPs designed in the present study were suitable as an effective gene carrier for pZNF580.

3.9. NPs/pZNF580 Complexes for Actively Targeting of ECs. When NPs/pZNF580 complexes were cultured with ECs and SMCs in the growth medium, REDV peptide was specifically recognized by receptors (integrin $\alpha_4\beta_1$) on the cytomembrane surface of ECs, which was expressed in abundance by ECs but not by other cell types.[59] The special recognition process of REDV peptide and receptor was shown in Figure 4. Thus, the actively targeting complexes can be effectively transported into cells by endocytosis. After escape from endolysosome and entrance into cell nucleus, pZNF580 could effectively express in the nucleus. In this way, the proliferation of ECs could be greatly promoted.

In the coculture system, cells were transfected with NPs/pZNF580 complexes for another 24 h. After fixing and dyeing, images of different cells with specificity fluorescence were obtained. All of the cell nuclei of ECs and SMCs were dyed blue by DAPI (Figure 11 b). In a comparison with SMCs that were dyed red by RBITC (Figure 11 d), it was obviously found that the number of ECs (dyed into green by FITC) was much larger than that of SMCs (Figure 11 c). These results demonstrated that the NPs/pZNF580 could be selected specifically by ECs, and the proliferation of ECs was promoted greatly by the overexpression of ZNF580 gene in the coculture medium.

In the coculture system, the actively targeting NPs/pZNF580 complexes were adhered selectively through recognition of

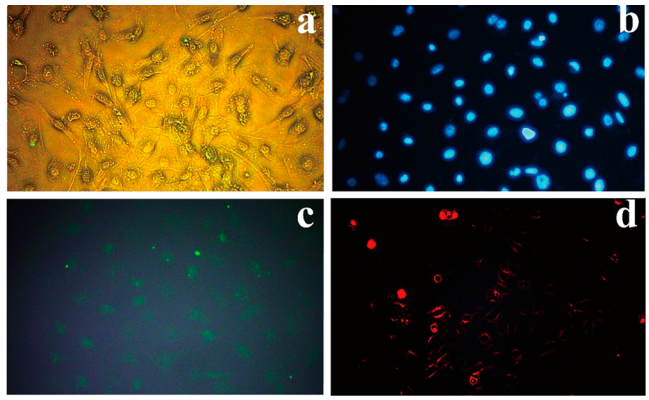

Figure 11. Immunofluorescence images of ECs and SMCs transfected by REDV-*g*-PEI-*g*-P(LA-*co*-GA)-*g*-PEI-*g*-$REDV_1$ based NPs/pZNF580 complexes in the coculture system: (a) image of ECs and SMCs coculture system after 24 h, (b) cell nucleus images of ECs and SMCs dyed by DAPI, (c) images of cultured ECs by anti-CD31 antibody (FITC labeled CD31), and (d) images of cultured SMCs by anti-α-SMA antibody (RBITC labeled α-SMA).

REDV ligands and $\alpha_4\beta_1$ receptors, and then transfected effectively into ECs. After the overexpression of ZNF580 protein, the proliferation of ECs was promoted greatly. Meanwhile, these NPs/pZNF580 complexes had the selective ability for ECs; namely, they could be recognized specifically and adhered to efficiently by the $\alpha_4\beta_1$ integrin receptor which only located on the membrane surface of ECs.[59] Therefore, the probability of the complexes entering into the SMCs reduced greatly. Thus, these targeting NPs/pZNF580 complexes prepared in the present paper could be specifically selected by ECs, and only promote their proliferation.

4. DISCUSSION

Cardiovascular diseases have become one of the main causes of death in the world. For treatment of these diseases, artificial blood vessels are usually used to replace the diseased arteries or bypass an occlusion in a blood vessel. However, high occurrence of restenosis and thrombosis limits their application as small diameter artificial blood vessels.[60] Rapid endothelialization is an effective strategy to create an antithrombotic artificial blood vessel surface. Many methods have been investigated to enhance the endothelialization of implants. For artificial blood vessels, cell seeding is one of the fascinating strategies. Therefore, endothelial progenitor cells have been usually used in cell seeding strategy,[61] because they can regenerate the function of ischemic organs by stimulating the re-endothelialization of injured blood vessels.[62] In addition, antibodies and peptides have also been widely used in the modification of artificial blood vessels.[21]

In order to endow the surface of artificial blood vessels with special EC adhesion function, REDV, CAG, and SVVYGLR peptides have been widely investigated to modify biomaterial surface *in vitro* and *in vivo*.[63,64] Among these peptides, REDV peptide could be recognized and adhered by $\alpha_4\beta_1$ integrin on the membrane of ECs. REDV peptide modified implants have been demonstrated to have important application prospects because of the enhancement of selectivity of ECs over SMCs.[65]

Recently, several modified PEI gene carriers for the delivery of ZNF580 gene have been reported by our research group.[66] The proliferation and migration of ECs are promoted by the complexes of modified PEI gene carrier/pZNF580.[25,26,67]

DOI: 10.1021/acsami.5b06286
ACS Appl. Mater. Interfaces 2015, 7, 20389−20399

Nevertheless, these complexes could not be selectively adhered by ECs in the coculture system. Therefore, it is necessary to develop an actively targeting gene delivery system to specifically transfect ECs in the coculture system.

The special adhesion of REDV peptide gives us an inspiration to prepare targeting gene carriers for ECs. With great interest, we synthesized a series of biodegradable block copolymers with EC-targeting functional peptide, subsequently prepared the EC-targeting NPs from these copolymers. Herein, these copolymers were synthesized from MMD, L-LA, and GA by ring-opening polymerization and then grafting reaction of PEI and CREDVW peptide. MMD and GA were used to adjust the degradation of the copolymers. The hydrophobic cores of NPs were formed by P(LA-*co*-GA) or P(LA-*co*-GA-*co*-MMD) segments, which provided physically cross-linking points for PEI chains. On the surface of NPs, REDV peptide as the ligand could be recognized by integrin receptors.

The zeta potential of targeting NPs prepared in the present paper ranged from 24.1 ± 0.9 to 31.6 ± 0.6 mV. Owing to the positively charged surface of the NPs, they could compact pZNF580 to form NPs/pZNF580 complexes. The size of the NPs ranged from 66.3 ± 10.5 to 75.1 ± 6.1 nm, which is beneficial for endocytosis by ECs.[68] Because of several targeting peptides on the surface of NPs/pZNF580 complexes, these targeting complexes were preferentially selected and adhered to by ECs in the coculture system. However, due to the electrostatic interaction between positively charged NPs/pZNF580 complexes and negatively charged cell membranes, in the control group, NPs without actively targeting peptides could not be selected and adhered specifically by both ECs and SMCs in coculture system.[69]

After the release of pZNF580 gene from NPs/pZNF580 complexes in the transfected ECs, pZNF580 gene finally expressed in the nucleus (Figure 4). The results of the transwell assay showed that the migration ability of ECs transfected by targeting NPs/pZNF580 complexes was promoted significantly by the expression of pZNF580 gene.

Furthermore, NPs and their complexes were prepared from REDV peptide grafted triblock copolymer of PEI-*g*-P(LA-*co*-GA-*co*-MMD)-*g*-PEI and PEI-*g*-P(LA-*co*-GA)-*g*-PEI, and condensation with pZNF580, respectively. The nontargeting complexes were also prepared and used as control group to evaluate the proliferation and migration of ECs in the coculture system of ECs and SMCs. Compared with an actively targeting NPs/pZNF580 gene delivery system, the nontargeting NPs/pZNF580 complexes could not be selected specifically by ECs over SMCs. The targeting NPs/pZNF580 complexes could be specifically selected by ECs; thus, they could promote the proliferation of ECs. Therefore, these actively targeting NPs/pZNF580 complexes might be used for efficient proliferation and migration of ECs, and show great potential for rapid endothelialization of artificial blood vessels.

5. CONCLUSIONS

We reported a strategy for proliferation and migration of ECs based on actively targeting NPs/pZNF580 complexes, which exhibited outstanding endothelial cell targeting performance with low cytotoxicity. The excellent endothelial cell selective performance enabled the proliferation and migration of ECs in the coculture system by actively targeting transfection with these complexes. Therefore, the actively targeting NPs/pZNF580 complexes should have great potential application for rapid endothelialization of artificial blood vessels.

■ ASSOCIATED CONTENT

Supporting Information

The Supporting Information is available free of charge on the ACS Publications website at DOI: 10.1021/acsami.5b06286.

Synthesis and characterization details, including fluorescence spectra and polymer characterizations, migration process, and cultured SMCs and ECs (PDF)

■ AUTHOR INFORMATION

Corresponding Authors

*Phone: +86-22-27401447. Fax: +86-022-27408829. E-mail: yakaifeng@tju.edu.cn.

*Phone: +86-22-27401447. Fax: +86-022-27408829. E-mail: renxiangkui@tju.edu.cn.

Notes

The authors declare no competing financial interest.

■ ACKNOWLEDGMENTS

This work was supported by the National Natural Science Foundation of China (Grant 31370969), the International Cooperation from Ministry of Science and Technology of China (Grant 2013DFG52040), the Natural Science Foundation of Tianjin and Youth Science Foundation (14JCQNJC02900), and the Program of Introducing Talents of Discipline to Universities of China (Grant B06006).

■ REFERENCES

(1) Krawiec, J.; Vorp, D. Adult Stem Cell-Based Tissue Engineered Blood Vessels: A Review. *Biomaterials* **2012**, *33*, 3388−3400.

(2) Sun, M.; Deng, J.; Gao, C. The Correlation between Fibronectin Adsorption and Attachment of Vascular Cells on Heparinized Polycaprolactone Membrane. *J. Colloid Interface Sci.* **2015**, *448*, 231−237.

(3) Isenberg, B. C.; Williams, C.; Tranquillo, R. T. Small-Diameter Artificial Arteries Engineered in Vitro. *Circ. Res.* **2006**, *98*, 25−35.

(4) Burck, J.; Heissler, S.; Geckle, U.; Ardakani, M. F.; Schneider, R.; Ulrich, A. S.; Kazanci, M. Resemblance of Electrospun Collagen Nanofibers to Their Native Structure. *Langmuir* **2013**, *29*, 1562−1572.

(5) Wang, H.; Feng, Y.; Fang, Z.; Xiao, R.; Yuan, W.; Khan, M. Fabrication and Characterization of Electrospun Gelatin-Heparin Nanofibers as Vascular Tissue Engineering. *Macromol. Res.* **2013**, *21*, 860−869.

(6) Yang, J.; Lv, J.; Gao, B.; Zhang, L.; Yang, D.; Shi, C.; Guo, J.; Li, W.; Feng, Y. Modification of Polycarbonateurethane Surface with Poly (Ethylene Glycol) Monoacrylate and Phosphorylcholine Glyceraldehyde for Anti-Platelet Adhesion. Front. *Front. Chem. Sci. Eng.* **2014**, *8*, 188−196.

(7) Yuan, W.; Feng, Y.; Wang, H.; Yang, D.; An, B.; Zhang, W.; Khan, M.; Guo, J. Hemocompatible Surface of Electrospun Nanofibrous Scaffolds by ATRP Modification. *Mater. Sci. Eng., C* **2013**, *33*, 3644−3651.

(8) Wang, H.; Feng, Y.; Fang, Z.; Yuan, W.; Khan, M. Co-Electrospun Blends of PU and PEG as Potential Biocompatible Scaffolds for Small-Diameter Vascular Tissue Engineering. *Mater. Sci. Eng., C* **2012**, *32*, 2306−2315.

(9) Yang, J.; Lv, J.; Behl, M.; Lendlein, A.; Yang, D.; Zhang, L.; Shi, C.; Guo, J.; Feng, Y. Functionalization of Polycarbonate Surfaces by Grafting PEG and Zwitterionic Polymers with a Multicomb Structure. *Macromol. Biosci.* **2013**, *13*, 1681−1688.

(10) Wang, H.; Feng, Y.; An, B.; Zhang, W.; Sun, M.; Fang, Z.; Yuan, W.; Khan, M. Fabrication of PU/PEGMA Crosslinked Hybrid Scaffolds by in Situ UV Photopolymerization Favoring Human Endothelial Cells Growth for Vascular Tissue Engineering. *J. Mater. Sci.: Mater. Med.* **2012**, *23*, 1499−1510.

DOI: 10.1021/acsami.5b06286
ACS Appl. Mater. Interfaces 2015, 7, 20389−20399

(11) Wang, H.; Feng, Y.; Zhao, H.; Lu, J.; Guo, J.; Behl, M.; Lendlein, A. Controlled Heparin Release from Electrospun Gelatin Fibers. *J. Controlled Release* **2011**, *152*, e28−29.
(12) Shi, C.; Yuan, W.; Khan, M.; Li, Q.; Feng, Y.; Yao, F.; Zhang, W. Hydrophilic PCU Scaffolds Prepared by Grafting PEGMA and Immobilizing Gelatin to Enhance Cell Adhesion and Proliferation. *Mater. Sci. Eng., C* **2015**, *50*, 201−209.
(13) Gao, B.; Feng, Y.; Lu, J.; Zhang, L.; Zhao, M.; Shi, C.; Khan, M.; Guo, J. Grafting of Phosphorylcholine Functional Groups on Polycarbonate Urethane Surface for Resisting Platelet Adhesion. *Mater. Sci. Eng., C* **2013**, *33* (5), 2871−2878.
(14) Lu, J.; Feng, Y.; Gao, B.; Guo, J. Grafting of a Novel Phosphorylcholine-Containing Vinyl Monomer onto Polycarbonateurethane Surfaces by Ultraviolet Radiation Grafting Polymerization. *Macromol. Res.* **2012**, *20*, 693−702.
(15) Khan, M.; Yang, J.; Shi, C.; Feng, Y.; Zhang, W.; Gibney, K.; Tew, G. N. Surface Modification of Polycarbonate Urethane with Zwitterionic Polynorbornene via Thiol-eneClick-Reactionto Facilitate Cell Growth and Proliferation. *Macromol. Mater. Eng.* **2015**, *300*, 802−809.
(16) Yu, L.; Hao, X. F.; Li, Q.; Shi, C. C.; Feng, Y. K. Electrospun PLGA/SF Modified with Electrosprayed Microparticles: A Novel Biomimetic Composite Scaffold for Vascular Tissue Engineering. *Adv. Mater. Res.* **2014**, *1015*, 336−339.
(17) Zhou, W.; Feng, Y.; Yang, J.; Fan, J.; Lv, J.; Zhang, L.; Guo, J.; Ren, X.; Zhang, W. Electrospun Scaffolds of Silk Fibroin and Poly(lactide-co-glycolide) for Endothelial Cell Growth. *J. Mater. Sci.: Mater. Med.* **2015**, *26*, 5386.
(18) Ren, X. K.; Feng, Y. K.; Guo, J. T.; Wang, H. X.; Li, Q.; Yang, J.; Hao, X. F.; Lv, J.; Ma, N.; Li, W. Z. Surface Modification and Endothelialization of Biomaterials as Potential Scaffolds for Vascular Tissue Engineering Application. *Chem. Soc. Rev.* **2015**, *44*, 5680−5742.
(19) Qi, P. K.; Maitz, M. F.; Huang, N. Surface Modification of Cardiovascular Materials and Implants. *Surf. Coat. Technol.* **2013**, *233*, 80−90.
(20) Mahara, A.; Somekawa, S.; Kobayashi, N.; Hirano, Y.; Kimura, Y.; Fujisato, T.; Yamaoka, T. Tissue-Engineered Acellular Small Diameter Long-Bypass Grafts with Neointima-Inducing Activity. *Biomaterials* **2015**, *58*, 54−62.
(21) Zheng, W.; Wang, Z.; Song, L.; Zhao, Q.; Zhang, J.; Li, D.; Wang, S.; Han, J.; Zheng, X. L.; Yang, Z.; Kong, D. Endothelialization and Patency of RGD-Functionalized Vascular Grafts in a Rabbit Carotid Artery Model. *Biomaterials* **2012**, *33*, 2880−2891.
(22) Massia, S. P.; Hubbell, J. A. Vascular Endothelial Cell Adhesion and Spreading Promoted by the Peptide REDV of the IIICS Region of Plasma Fibronectin is Mediated by Integrin $\alpha 4\,\beta 1$. *J. Biol. Chem.* **1992**, *267*, 14019−14026.
(23) Lin, Q.; Hou, Y.; Ren, K. F.; Ji, J. Selective Endothelial Cells Adhesion to Arg-Glu-Asp-Val Peptide Functionalized Polysaccharide Multilayer. *Thin Solid Films* **2012**, *520*, 4971−4978.
(24) Wei, Y.; Ji, Y.; Xiao, L. L.; Lin, K.; Xu, J. P.; Ren, K. F.; Ji, J. Surface Engineering of Cardiovascular Stent with Endothelial Cell Selectivity for in Vivo Re-Endothelialisation. *Biomaterials* **2013**, *34*, 2588−2599.
(25) Shi, C.; Yao, F.; Li, Q.; Khan, M.; Ren, X.; Feng, Y.; Huang, J.; Zhang, W. Regulation of the Endothelialization by Human Vascular Endothelial Cells by ZNF580 Gene Complexed with Biodegradable Microparticles. *Biomaterials* **2014**, *35*, 7133−7145.
(26) Shi, C.; Yao, F.; Huang, J.; Han, G.; Li, Q.; Khan, M.; Feng, Y.; Zhang, W. Proliferation and Migration of Human Vascular Endothelial Cells Mediated by ZNF580 Gene Complexed with mPEG-b-P(MMD-co-GA)-g-PEI Microparticles. *J. Mater. Chem. B* **2014**, *2*, 1825−1837.
(27) Wang, D.; Fei, B.; Halig, L. V.; Qin, X.; Hu, Z.; Xu, H.; Wang, Y. A.; Chen, Z.; Kim, S.; Shin, D. M.; Chen, Z. G. Targeted Iron-Oxide Nanoparticle for Photodynamic Therapy and Imaging of Head and Neck Cancer. *ACS Nano* **2014**, *8*, 6620−6632.
(28) Kang, J. H.; Tachibana, Y.; Kamata, W.; Mahara, A.; Harada-Shiba, M.; Yamaoka, T. Liver-Targeted siRNA Delivery by Polyethylenimine (PEI)-Pullulan Carrier. *Bioorg. Med. Chem.* **2010**, *18*, 3946−3950.
(29) Lee, M.-Y.; Park, S.-J.; Park, K.; Kim, K. S.; Lee, H.; Hahn, S. K. Target-Specific Gene Silencing of Layer-by-Layer Assembled Gold-Cysteamine/siRNA/PEI/HA Nanocomplex. *ACS Nano* **2011**, *5*, 6138−6147.
(30) Jiang, L.; Li, L.; He, X.; Yi, Q.; He, B.; Cao, J.; Pan, W.; Gu, Z. Overcoming Drug-Resistant Lung Cancer by Paclitaxel Loaded Dual-Functional Liposomes with Mitochondria Targeting and pH-Response. *Biomaterials* **2015**, *52*, 126−139.
(31) Zhong, Y.; Wang, C.; Cheng, R.; Cheng, L.; Meng, F.; Liu, Z.; Zhong, Z. cRGD-Directed, NIR-Responsive and Robust AuNR/PEG-PCL Hybrid Nanoparticles for Targeted Chemotherapy of Glioblastoma In Vivo. *J. Controlled Release* **2014**, *195*, 63−71.
(32) Wang, X.; Yang, C.; Zhang, Y.; Zhen, X.; Wu, W.; Jiang, X. Delivery of Platinum(IV) Drug to Subcutaneous Tumor and Lung Metastasis Using Bradykinin-Potentiating Peptide-Decorated Chitosan Nanoparticles. *Biomaterials* **2014**, *35*, 6439−6453.
(33) Yao, F.; Hu, H.; Xu, S.; Huo, R.; Zhao, Z.; Zhang, F.; Xu, F. Preparation and Regulating Cell Adhesion of Anion-Exchangeable Layered Double Hydroxide Micropatterned Arrays. *ACS Appl. Mater. Interfaces* **2015**, *7*, 3882−3887.
(34) Wang, H.; Feng, Y.; Yang, J.; Guo, J.; Zhang, W. Targeting REDV Peptide Functionalized Polycationic Gene Carrier for Enhancing the Transfection and Migration Capability of Human Endothelial Cells. *J. Mater. Chem. B* **2015**, *3*, 3379−3391.
(35) Hao, X.; Li, Q.; Lv, J.; Yu, L.; Ren, X.; Zhang, L.; Feng, Y.; Zhang, W. CREDVW-Linked Polymeric Micelles As a Targeting Gene Transfer Vector for Selective Transfection and Proliferation of Endothelial Cells. *ACS Appl. Mater. Interfaces* **2015**, *7*, 12128−12140.
(36) Sierzchala, A. B.; Dellinger, D. J.; Betley, J. R.; Wyrzykiewicz, T. K.; Yamada, C. M.; Caruthers, M. H. Solid-Phase Oligodeoxynucleotide Synthesis: A Two-Step Cycle Using Peroxy Anion Deprotection. *J. Am. Chem. Soc.* **2003**, *125*, 13427−13441.
(37) Singha, N. K.; Gibson, M. I.; Koiry, B. P.; Danial, M.; Klok, H. A. Side-Chain Peptide-Synthetic Polymer Conjugates via Tandem "Ester-Amide/Thiol-Ene" Post-Polymerization Modification of Poly(Pentafluorophenyl Methacrylate) Obtained Using ATRP. *Biomacromolecules* **2011**, *12*, 2908−2913.
(38) Feng, Y.; Zhao, H.; Behl, M.; Lendlein, A.; Guo, J.; Yang, D. Grafting of Poly(Ethylene Glycol) Monoacrylates on Polycarbonateurethane by UV Initiated Polymerization for Improving Hemocompatibility. *J. Mater. Sci.: Mater. Med.* **2013**, *24*, 61−70.
(39) Jeon, O.; Lee, S.; Kim, S. H.; Lee, Y. M.; Kim, Y. H. Synthesis and Characterization of Poly(L-Lactide)-Poly(ε-caprolactone) Multiblock Copolymers. *Macromolecules* **2003**, *36*, 5585−5592.
(40) Gargouri, M.; Sapin, A.; Arica-Yegin, B.; Merlin, J. L.; Becuwe, P.; Maincent, P. Photochemical Internalization for pDNA Transfection: Evaluation of Poly(D,L-Lactide-co-Glycolide) and Poly(ethylenimine) Nanoparticles. *Int. J. Pharm.* **2011**, *403*, 276−284.
(41) Cheng, Q.; Huang, Y.; Zheng, H.; Wei, T.; Zheng, S.; Huo, S.; Wang, X.; Du, Q.; Zhang, X.; Zhang, H. Y.; Liang, X. J.; Wang, C.; Tang, R.; Liang, Z. The Effect of Guanidinylation of PEGylated Poly(2-Aminoethyl Methacrylate) on the Systemic Delivery of siRNA. *Biomaterials* **2013**, *34*, 3120−3131.
(42) Ren, D.; Wang, H.; Liu, J.; Zhang, M.; Zhang, W. ROS-Induced ZNF580 Expression: A Key Role for H2O2/NF-κB Signaling Pathway in Vascular Endothelial Inflammation. *Mol. Cell. Biochem.* **2012**, *359*, 183−191.
(43) Zubair, M.; Ekholm, A.; Nybom, H.; Renvert, S.; Widen, C.; Rumpunen, K. Effects of Plantago Major L. Leaf Extracts on Oral Epithelial Cells in a Scratch Assay. *J. Ethnopharmacol.* **2012**, *141*, 825−830.
(44) Hung, W.; Chang, H. Indole-3-Carbinol Inhibits SP1-Induced Matrix Metalloproteinase-2 Expression to Attenuate Migration and Invasion of Breast Cancer Cells. *J. Agric. Food Chem.* **2009**, *57*, 76−82.
(45) Sun, H.; Wei, S.; Xu, R.; Xu, P.; Zhang, W. Sphingosine-1-Phosphate Induces Human Endothelial VEGF and MMP-2

DOI: 10.1021/acsami.5b06286
ACS Appl. Mater. Interfaces 2015, 7, 20389−20399

Production via Transcription Factor ZNF580: Novel Insights into Angiogenesis. *Biochem. Biophys. Res. Commun.* **2010**, *395*, 361−366.
(46) Farooq, A.; Whitehead, D.; Azzawi, M. Attenuation of Endothelial-Dependent Vasodilator Responses, Induced by Dye-Encapsulated Silica Nanoparticles, in Aortic Vessels. *Nanomedicine (London, U. K.)* **2014**, *9*, 413−425.
(47) Li, X.; Kong, X.; Shi, S.; Gu, Y.; Yang, L.; Guo, G.; Luo, F.; Zhao, X.; Wei, Y.; Qian, Z. Biodegradable MPEG-g-Chitosan and Methoxy Poly(ethylene glycol)-b-Poly(ε-caprolactone) Composite Films: Part 1. Preparation and Characterization. *Carbohydr. Polym.* **2010**, *79*, 429−436.
(48) Sen Karaman, D.; Gulin-Sarfraz, T.; Hedstrom, G.; Duchanoy, A.; Eklund, P.; Rosenholm, J. M. Rational Evaluation of the Utilization of PEG-PEI Copolymers for the Facilitation of Silica Nanoparticulate Systems in Biomedical Applications. *J. Colloid Interface Sci.* **2014**, *418*, 300−310.
(49) Hong, W.; Chen, D.; Jia, L.; Gu, J.; Hu, H.; Zhao, X.; Qiao, M. Thermo- and pH-Responsive Copolymers Based on PLGA-PEG-PLGA and Poly(L-histidine): Synthesis and in Vitro Characterization of Copolymer Micelles. *Acta Biomater.* **2014**, *10*, 1259−1271.
(50) Shuai, X.; Merdan, T.; Unger, F.; Wittmar, M.; Kissel, T. Novel Biodegradable Ternary Copolymershy-PEI-g-PCL-b-PEG: Synthesis, Characterization, and Potential as Efficient Nonviral Gene Delivery Vectors. *Macromolecules* **2003**, *36*, 5751−5759.
(51) Du, F.; Ye, W.; Gu, Z.; Yang, J. Synthesis and in Vitro Degradation of Copolymers of Glycolide and 6 (R,S)-Methylmorpholine-2,5-Dione. *J. Appl. Polym. Sci.* **1997**, *63*, 643−650.
(52) He, Y.; Cheng, G.; Xie, L.; Nie, Y.; He, B.; Gu, Z. Polyethyleneimine/DNA polyplexes with Reduction-Sensitive Hyaluronic Acid Derivatives Shielding for Targeted Gene Delivery. *Biomaterials* **2013**, *34*, 1235−1245.
(53) Evans, C. W.; Fitzgerald, M.; Clemons, T. D.; House, M. J.; Padman, B. S.; Shaw, J. A.; Saunders, M.; Harvey, A. R.; Zdyrko, B.; Luzinov, I.; Silva, G. A.; Dunlop, S. A.; Iyer, K. S. Multimodal Analysis of PEI-Mediated Endocytosis of Nanoparticles in Neural Cells. *ACS Nano* **2011**, *5*, 8640−8648.
(54) Zhang, Q.; Yi, W.; Wang, B.; Zhang, J.; Ren, L.; Chen, Q. M.; Guo, L.; Yu, X. Q. Linear Polycations by Ring-Opening Polymerization as Non-Viral Gene Delivery Vectors. *Biomaterials* **2013**, *34*, 5391−5401.
(55) Elfinger, M.; Pfeifer, C.; Uezguen, S.; Golas, M. M.; Sander, B.; Maucksch, C.; Stark, H.; Aneja, M. K.; Rudolph, C. Self-Assembly of Ternary Insulin-Polyethylenimine (PEI)-DNA Nanoparticles for Enhanced Gene Delivery and Expression in Alveolar Epithelial Cells. *Biomacromolecules* **2009**, *10*, 2912−2920.
(56) Lobovkina, T.; Jacobson, G. B.; Gonzalez-Gonzalez, E.; Hickerson, R. P.; Leake, D.; Kaspar, R. L.; Contag, C. H.; Zare, R. N. In Vivo Sustained Release of siRNA From Solid Lipid Nanoparticles. *ACS Nano* **2011**, *5*, 9977−9983.
(57) Jorge, A. F.; Dias, R. S.; Pereira, J. C.; Pais, A. A. DNA Condensation by pH-Responsive Polycations. *Biomacromolecules* **2010**, *11*, 2399−2406.
(58) Hägglund, B.; Sandberg, G. Effect of L-Alanine and Some Other Amino Acids on Thymocyte Proliferation in Vivo. *Immunobiology* **1993**, *188*, 62−69.
(59) Liu, Y.; Tan, T. T. Y.; Yuan, S. J.; Choong, C. Multifunctional P(PEGMA)-REDV Conjugated Titanium Surfaces for Improved Endothelial Cell Selectivity and Hemocompatibility. *J. Mater. Chem. B* **2013**, *1*, 157−167.
(60) Avci-Adali, M.; Ziemer, G.; Wendel, H. P. Induction of EPC Homing on Biofunctionalized Vascular Grafts for Rapid in Vivo self-Endothelialization-A Review of Current Strategies. *Biotechnol. Adv.* **2010**, *28*, 119−129.
(61) Vartanian, K. B.; Kirkpatrick, S. J.; McCarty, O. J.; Vu, T. Q.; Hanson, S. R.; Hinds, M. T. Distinct Extracellular Matrix Microenvironments of progenitor and Carotid Endothelial Cells. *J. Biomed. Mater. Res., Part A* **2009**, *91*, 528−539.
(62) Griese, D. P.; Ehsan, A.; Melo, L. G.; Kong, D.; Zhang, L.; Mann, M. J.; Pratt, R. E.; Mulligan, R. C.; Dzau, V. J. Isolation and Transplantation of Autologous Circulating Endothelial Cells into Denuded Vessels and Prosthetic Grafts: Implications for Cell-Based Vascular Therapy. *Circulation* **2003**, *108*, 2710−2715.
(63) Castellanos, M. I.; Zenses, A. S.; Grau, A.; Rodriguez-Cabello, J. C.; Gil, F. J.; Manero, J. M.; Pegueroles, M. Biofunctionalization of REDV Elastin-Like Recombinamers Improves Endothelialization on CoCr Alloy Surfaces for Cardiovascular Applications. *Colloids Surf., B* **2015**, *127*, 22−32.
(64) Khan, M.; Yang, J.; Shi, C.; Lv, J.; Feng, Y. Surface Tailoring for Selective Endothelialization and Platelet Inhibition via a Combination of SI-ATRP and Click-Chemistry Using Cys-Ala-Gly-Peptide. *Acta Biomater.* **2015**, *20*, 69−81.
(65) Wei, Y.; Ji, Y.; Xiao, L.; Lin, Q.; Ji, J. Different Complex Surfaces of Polyethyleneglycol (PEG) and REDV Ligand to Enhance the Endothelial Cells Selectivity over Smooth Muscle Cells. Colloids Surf. *Colloids Surf., B* **2011**, *84*, 369−378.
(66) Lv, J.; Hao, X.; Yang, J.; Feng, Y.; Behl, M.; Lendlein, A. Self-Assembly of Polyethylenimine-Modified Biodegradable Complex Micelles as Gene Transfer Vector for Proliferation of Endothelial Cells. *Macromol. Chem. Phys.* **2014**, *215*, 2463−2472.
(67) Li, Q.; Shi, C.; Zhang, W.; Behl, M.; Lendlein, A.; Feng, Y. Nanoparticles Complexed with Gene Vectors to Promote Proliferation of Human Vascular Endothelial Cells. *Adv. Healthcare Mater.* **2015**, *4*, 1225−1235.
(68) Qiu, L.; Chen, T.; Öçsoy, I.; Yasun, E.; Wu, C.; Zhu, G.; You, M.; Han, D.; Jiang, J.; Yu, R.; Tan, W. A Cell-Targeted, Size-Photocontrollable, Nuclear-Uptake Nanodrug Delivery System for Drug-Resistant Cancer Therapy. *Nano Lett.* **2015**, *15*, 457−463.
(69) Xu, C.; Yang, D.; Mei, L.; Lu, B.; Chen, L.; Li, Q.; Zhu, H.; Wang, T. Encapsulating Gold Nanoparticles or Nanorods in Graphene Oxide Shells as a Novel Gene Vector. *ACS Appl. Mater. Interfaces* **2013**, *5*, 2715−2724.

DOI: 10.1021/acsami.5b06286
ACS Appl. Mater. Interfaces 2015, 7, 20389−20399